Engineering Structures 179 (2019) 310–320

Contents lists available at ScienceDirect

Engineering Structures

journal homepage: www.elsevier.com/locate/engstruct

Buckling of shells with special shapes with corrugated middle surfaces – FEM study

K. Sowiński

Institute of Applied Mechanics, Faculty of Mechanical Engineering and Management, Poznan University of Technology, ul. Jana Pawła II 24, 60-965 Poznan, Poland

ARTICLE INFO

Keywords:
Shell structures
Corrugated shells
Buckling
Structural stability
Finite element method

ABSTRACT

The problem of elastic stability of the shells with special shapes with corrugated middle surfaces under external pressure is debated in the presented paper. Solution of the problem is based on FEM study. Corrugated barrelled, pseudo-barrelled, and cylindrical shells of constant mass are considered. Geometrical modification of the middle surface geometry is based on sine wave along principal directions. Middle surface of the corrugated shells are described referring to differential geometry of surfaces by parametric functions in three-dimensional Euclidean space. Linear and nonlinear buckling analyses are conducted. Examples of buckling modes are presented, which differ significantly from those typical for shells of revolution with positive or zero Gaussian curvature. It is proven that corrugation may lead to serious increase or decrease of critical load for all types of presented shells.

1. Introduction

Continuous search for optimal technical solutions creates the need to develop more efficient structures. Due to the wide spectrum of shells applications in the industry, many authors devoted their efforts towards description of stress state and stability analysis of shells. In conjunction with thin-walled nature of those structures the most vivid branch of structural analysis of shells is stability problem. Among many monographs concerning structural stability one can distinguish the following: [1–5]. There are also many papers devoted to analytical and numerical solutions of buckling behaviour, concerning shells with unique geometrical forms. Due to practical limitations, shapes are usually narrowed to cylinders [6,7], spheres [8], and cones [9,10]. However, more often further complex shapes are being topics of consideration, for example: barrels [11], pseudo-barrels [12], pseudo-spheres [13], bi-segmented spherical shells [14], multi-segmented spherical shells [15], clothoidal-spherical shells [16] and egg-shaped shells [17]. Zingoni [18] presented a review work concerning liquid-containment shells of revolution including non-conventional shapes. Additionally various shell panels are being objects of intensive studies. Post-buckling problems of multiple shell panels are discussed in [19,20] using higher-order theories.

The most effective way of increasing load-carrying ability of shell structures is modification of their geometrical form. This fact can be assumed due to the number of diverse types of shells shapes that have been developed in recent decades. In this work the effect of corrugation of shells with positive, negative, and zero Gaussian curvature on stability is considered. Some of corrugated structures, mainly longitudinally corrugated cylinders have been already studied. Malinowski et al. [21] presented the buckling problem of sandwich cylindrical shell with corrugated main core, subjected to uniformly distributed external pressure. Iwicki et al. [22,23] investigated numerous stability problems of silos composed of corrugated sheets and columns. Jongpradist et al. [24] considered a corrugated food can design in terms of stability and strength, by experimental studies and response surface method. Dickson et al. [25] performed an analytical study of buckling problem of ring-stiffened corrugated cylinders and compared results with experimental data. Liu et al. [26] studied numerically the problem of axial-impact on meridionally corrugated tubes with a view to improve the energy absorption aspect of standard circular tubes. Hao et al. [27,28] performed an analytical study to resolve a similar problem considering progressive buckling and dynamic response of such structures. The Authors verified the analytical solution with a numerical FEM study. Ghazijahani et al. [29] performed an experimental study on equivalent structures and compared obtained results with theoretical predictions. Ning and Pellegrino [30] extensively described the problem of axially compressed, circumferentially corrugated cylindrical shells. Malek [31] et al. investigated the effect of corrugation along two directions of the surface of barrelled vault. The authors have proven such modification can lead to a great increase of the buckling load. Malek and Williams [32] presented conceptual design of corrugated plates and shells. Using analytical approach, a closed-form solution of equilibrium state of such structures was obtained.

The study involves comparison of critical load for smooth and corrugated shells of constant mass. Applied corrugations are introduced to potentially increase load-carrying ability of selected shell structures. Those are assumed to be homogeneous, isotropic, and of constant thickness t. In terms of real-world applications, corrugated shells are extensively used to achieve lightweight structures with increased load-carrying abilities comparing to non-corrugated structures. Potential

https://doi.org/10.1016/j.engstruct.2018.10.055
Received 10 July 2018; Received in revised form 31 August 2018; Accepted 22 October 2018

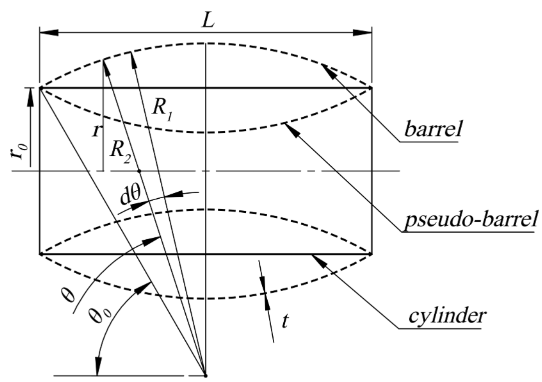

Fig. 1. Geometry of shells with special shapes.

applications of corrugated shells loaded with external pressure are following: pressure vessels, liquid storage tanks (draining process), underground tanks, cores of multi-layered shells, hulls of submersible vehicles, silos, road culverts and civil engineering structures. Such geometrical modification will be applied to cylindrical, barrelled, and pseudo-barrelled structures, hereinafter called collectively "shells with special shapes". This choice also implies similar mathematical description of their middle surfaces.

2. Geometrical description of shells with special shapes

Analysed shells of revolution with meridian of barrelled and pseudo-barrelled shell printed in dashed lines are presented in Fig. 1. Barrelled structures are shells of positive Gaussian curvature $K > 0$, whereas pseudo-barrels are characterised by negative Gaussian curvature $K < 0$. Cylindrical shells are particular case of both structures mentioned above, where radius of meridional curve $R_1 \to \infty$, thus $K = 0$.

The geometrical relation for any surface of revolution is

$$\frac{d}{d\theta}(R_2 sin\theta) = R_1 cos\theta, \tag{1}$$

where $\theta_0 \leq \theta \leq \theta_0 - \pi$.

Considering above relation, for cylindrical shells angular coordinate must be $\theta_0 = \pi/2$. Length of the shell L is related with parameter θ_0 and meridional radius R_1 in the following formula:

$$L = 2R_1 cos\theta_0. \tag{2}$$

Radius parameter r and circumferential radius R_2 for barrelled and pseudo-barrelled shells are expressed correspondingly:

$$r = r_0 \pm R_1(sin\theta - sin\theta_0), \tag{3}$$

$$R_2 = \frac{r}{sin\theta}. \tag{4}$$

3. Geometrical description of shells with special shapes with corrugated middle surfaces

To analyse shells with special shapes with corrugated middle surfaces it is necessary to describe their modified geometry. Corrugation is defined as sine wave along principal curves, i.e. for the one of them or both simultaneously. The geometry of corrugated barrelled shell in both principal directions is presented in Fig. 2.

Sine waves must meet particular conditions to maintain consistency of geometrical description. Those conditions are: symmetry of the structure with respect to the yz plane, minimal numbers of half-waves m_0 and full-waves n_0 along principal directions. Minimal numbers of full-waves and half-waves ensure that corrugation is regular along principal directions, the symmetry implies that the number of half-waves along meridional direction must be odd. The above assumptions can be written in the following form:

$$m \geq m_0,\ \ m = 2m' + 1,\ \ m' = 1, 2, 3\cdots, \tag{5}$$

$$n \geq n_0,\ \ n = 2n',\ \ n' = 1, 2, 3\cdots, \tag{6}$$

where correspondingly: m, n – numbers of half-waves and full-waves in meridional and circumferential directions, m', n'– increments of half-waves and full-waves.

Since the analysed issue concerns FEM study, the digital model of the corrugated shells is required. Therefore, it is necessary to describe their geometry in Cartesian coordinate system, which is used by the most of modelling software. Corrugated principal curves for barrelled and pseudo-barrelled shells are defined by the following parametric functions:

$$f_\theta = \begin{cases} x(\theta) = (R_0 \pm A_\theta)cos\theta \\ z(\theta) = r_0 \pm (R_0 \pm A_\theta)sin\theta \mp R_0 sin\theta_0 \end{cases} \tag{7}$$

Analogously circumferential curve on the edge of the structure ($x = \pm L/2$) is given by the formula

$$f_\varphi = \begin{cases} y(\varphi) = (r_0 + A_\varphi)sin\varphi \\ z(\varphi) = (r_0 + A_\varphi)cos\varphi \end{cases}, \tag{8}$$

where:

$$A_\theta = A_m sin\left[\frac{\pi}{\pi - 2\theta_0}(2m' + 1)(\theta - \theta_0)\right], \tag{9}$$

$$A_\varphi = A_n sin[(n' + 2)\varphi], \tag{10}$$

denoting: A_m, A_n – amplitudes of sine waves along meridional and circumferential direction respectively (Fig. 2).

The above equations allow to define parametric equations describing middle surfaces of corrugated barrelled and pseudo-barrelled shells in three-dimensional space. Structures based on Eq. (11) are shown in Table 1.

$$\Omega = \begin{cases} x(\theta, \varphi) = (R_0 \pm A_\theta)cos\theta \\ y(\theta, \varphi) = [r_0 \pm (R_0 \pm A_\theta)sin\theta \mp R_0 sin\theta_0 + A_\varphi]sin\varphi \\ z(\theta, \varphi) = [r_0 \pm (R_0 \pm A_\theta)sin\theta \mp R_0 sin\theta_0 + A_\varphi]cos\varphi \end{cases} \tag{11}$$

Eq. (11) can also describe geometry of the corrugated cylindrical shell, assuming $R \to \infty$. Radii of the principal curves after corrugation are not constant anymore, therefore the shell corrugated in circumferential direction is not a shell of revolution. Moreover, corrugated shells are not surfaces of uniform Gaussian curvature. Such fact significantly complicates the analysed problem. To investigate the effect of corrugation on critical load, arbitrary forms of corrugation are considered. Meridional, circumferential or both corrugations simultaneously may occur. Due to that nine different types of shells are introduced: three basic shapes with three possible forms of corrugation. Mass of any shell can be expressed in following form

$$m_s = \rho t S, \tag{12}$$

where ρ – density of material, S– area of middle surface, t – thickness.

It is assumed that the factor which determines the mass of the shell is thickness t. Considering some particular type of material, surface area S must be determined. Referring to differential geometry of surfaces, area of parametric surface can be written in the formula

$$S = \int_0^{2\pi}\int_{\theta_0}^{\pi-\theta_0}\sqrt{\left(\frac{\partial y}{\partial\theta}\frac{\partial z}{\partial\varphi} - \frac{\partial y}{\partial\varphi}\frac{\partial z}{\partial\theta}\right)^2 + \left(\frac{\partial x}{\partial\theta}\frac{\partial z}{\partial\varphi} - \frac{\partial x}{\partial\varphi}\frac{\partial z}{\partial\theta}\right)^2 + \left(\frac{\partial x}{\partial\theta}\frac{\partial y}{\partial\varphi} - \frac{\partial x}{\partial\varphi}\frac{\partial y}{\partial\theta}\right)^2}\,d\theta d\varphi. \tag{13}$$

It follows from middle surface equation (Eq. (11)) and surface area equation (Eq. (13)) that further analytical calculations are futile. Approximate result of Eq. (13) can be achieved by numerical integration using appropriate software.

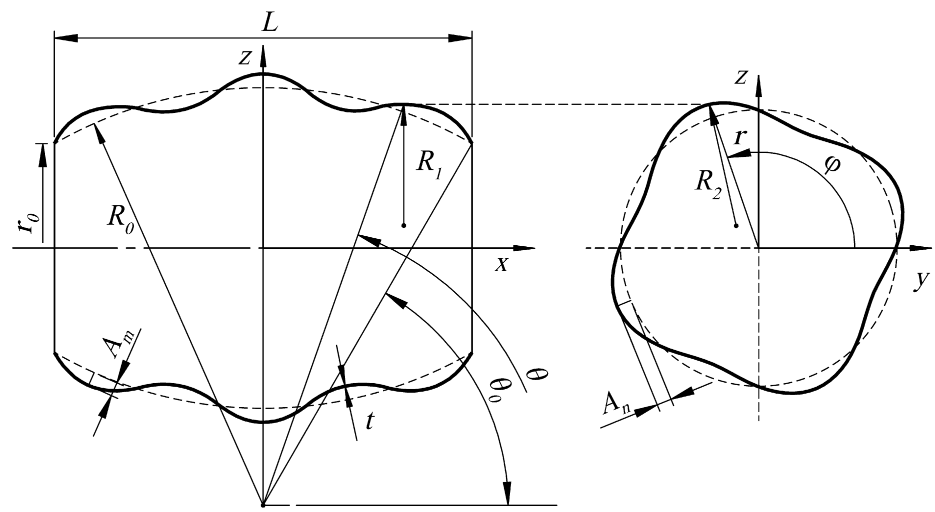

Fig. 2. Geometry of barrelled shell with corrugated middle surface.

4. Linear buckling

Numerical solution of stability analysis is achieved using Ansys 14.5 software by analysing first eigenvalue obtained from linear buckling analysis. FEM result for smooth, cylindrical shell was compared with an analytical solution. Analytical approach was described by non-linear equilibrium equations, solved by Galerkin method, assuming some special deflection function. In both cases buckling mode was represented by the six circumferential full-waves and one meridional half-wave. Critical load calculated analytically differed from numerical solution by 6.9%.

The most adequate approach to inspect effect of corrugation on structural stability is to compare critical load of corrugated shells to smooth shell of the same shape type, for example barrelled. For this reason the new parameter called relative critical load $\tilde{p}_{cr}$ is introduced

$$\tilde{p}_{cr} = \frac{p_{cr\,i}}{p_{cr\,0}}, \tag{14}$$

where $p_{cr\,i}$ – critical load of the shell with particular corrugation parameters, $p_{cr\,0}$ – critical load of smooth shell of the same type.

Digital model of corrugated shell was created using SolidWorks 2015 software. Fully parametric geometry of the structure is created using surface modelling. Model is verified by comparing the surface area values calculated by numerically integrating Eq. (13), with those calculated by the CAD software. As the applications of the corrugated shell structures can be wide, it is difficult to unambiguously decide about the values of geometrical parameters of the analysed structures. Following values are assumed: length $L = 2000$ mm and radius $r_0 = 500$ mm (Fig. 2). In addition, meridional radius for barrelled and pseudo-barrelled shell is $R_0 = 3000$ mm. Such values can be referred to many industrial pressure vessels and liquid storage tanks. In terms of mass and thickness it is desired to achieve a lightweight, economical structures by corrugating it. Mass of any structure is $m_s = 147.03$ kg, which corresponds to the cylindrical shell with a thickness of $t = 3$ mm. Dimensionless amplitudes are expressed by corrugation amplitudes A_m, A_n and radius r_0 in the following manner:

$$a_m = \frac{A_m}{r_0},\;\; a_n = \frac{A_n}{r_0}. \tag{15}$$

For the shells corrugated in one direction the following range of corrugation parameters are investigated:

$$m' = 1, 2, \cdots, 10,\;\; n' = 1, 2, \cdots, 15, \qquad a_m = 0.002, 0.004, \cdots, 0.05, \qquad a_n = 0.002, 0.004, \cdots, 0.05. \tag{16}$$

The shells corrugated in the both principal directions are considered to have constant dimensionless amplitudes $a_m = a_n = 0.05$. It is assumed that the dimensionless amplitudes for shells corrugated in one direction are changing by the increment of $a_i = 0.002$. Having in mind the above, one obtains total 2325 unique cases.

Table 1
Various corrugated shells described by Eq. (11).

	Barrelled shells			Pseudo-barrelled shells		
$n'\backslash m'$	0	5	10	0	5	10
0	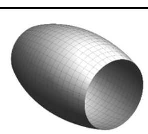	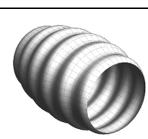	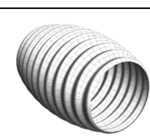	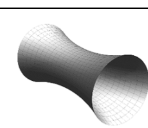	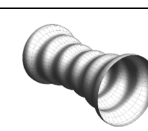	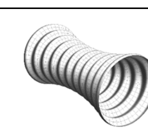
7	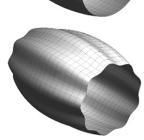	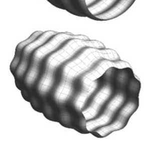	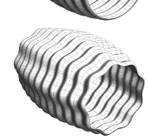	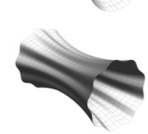	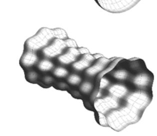	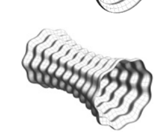
15	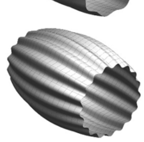	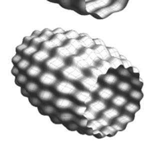	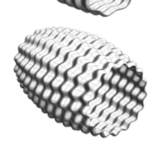	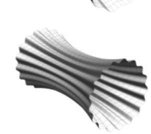	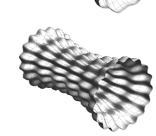	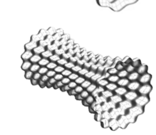

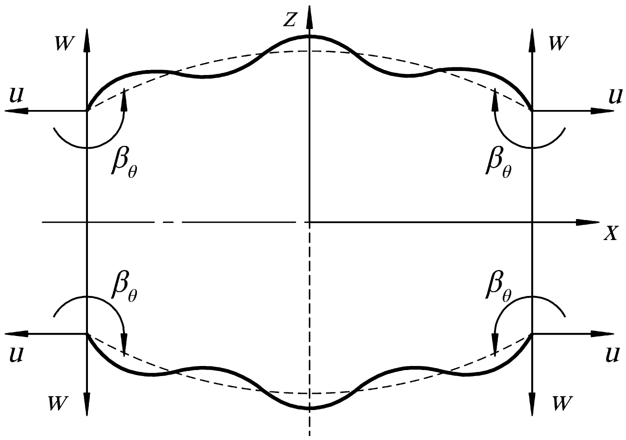

Fig. 3. Boundary conditions: u = 0, w = 0, $\beta_\theta \neq 0$.

Analysed geometrical modification in the form of corrugation highly restricts the number of boundary conditions possible to apply. This is due to the change in normal to the surface direction with different corrugation parameters. For the smooth cylindrical shell the direction mentioned above is parallel to z axis, while for the corrugated barrelled shell it can be roughly orthogonal to it. Therefore, allowing the structure to translate along normal to the surface direction one obtains divergent analyses cases. To avoid such discrepancies, all translations on the edge of the shell are blocked, while rotations remain free, according to Eurocode 3 [33] those conditions correspond to BC1f.

Referring to Fig. 3 boundary conditions can be written as follows:

$$u = 0, \quad w = 0, \quad \beta_\theta \neq 0.$$

The shell is loaded with uniform external pressure. Digital model of the corrugated shell is divided into a thin shell, four nodal elements named SHELL181 in the FEM software. Those finite elements have six degrees of freedom. The size of finite elements used in FEM must be based on mesh convergence, however, performing such analysis for each possible case is excessive and extremely time consuming. Considering the nature of finite element method it is essential to take into account the structures, for which a convergence condition may be achieved for the smallest geometrical size of finite elements. It is expected that analyses of shells with the greatest curvatures and surface areas may apply to the above statement. Consequently, mesh convergence analysis is performed for shells with maximum values of corrugation parameters in the range (nine convergence analyses in total). Example of such study is presented in Fig. 4. The material specification is the following: Poisson's ratio $\vartheta = 0.3$, Young's modulus $E = 2.05 \times 10^5$ MPa, density $\rho = 7.8$ g/cm^3.

Upon convergence analyses results, assumed discretization error tolerance and time needed to perform numerical calculations it has been assumed that size of finite elements is 15 mm for any considered shell. Decision is based on observation of the buckling modes and relative change of the critical load, which is less than assumed 1.5% error tolerance between 15 mm and 10 mm element size for every convergence analysis. Example of such study is presented in Fig. 4. If the mesh is regular it is more convenient to describe an FE model by number of elements along specified directions. For smooth shells it is 209 elements along circumferential edge for all of the shapes, 137 elements along the meridian of the barrelled or pseudo-barrelled shells and 134 elements along the meridian of the cylindrical shell. Obviously, those numbers increase with applied corrugations to maintain approximately constant size of the finite elements. Ranges of the FE models parameters values are presented in Table 2. In case of smooth

Table 2
Ranges of FE models parameters for all of the considered cases.

Number of finite elements n_e	Number of nodes n_n	Thickness t [mm]
$28006 \leq n_e \leq 60264$	$28215 \leq n_n \leq 60507$	$1.925 \leq t \leq 3.727$

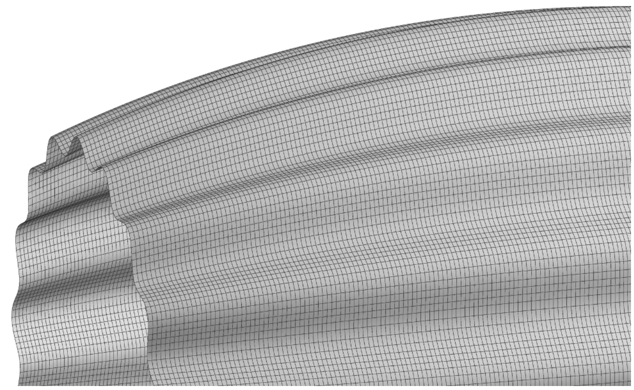

Fig. 5. Part of the meshed corrugated barrelled shell.

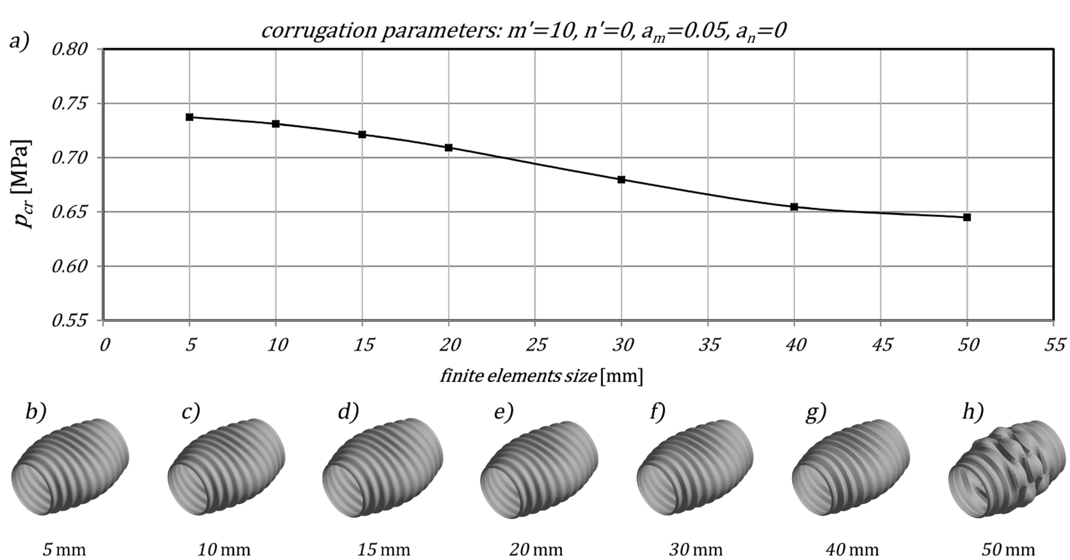

Fig. 4. Example of mesh convergence analysis. Change in critical load: a); buckled shells corresponding to specified finite elements size: b)–h).

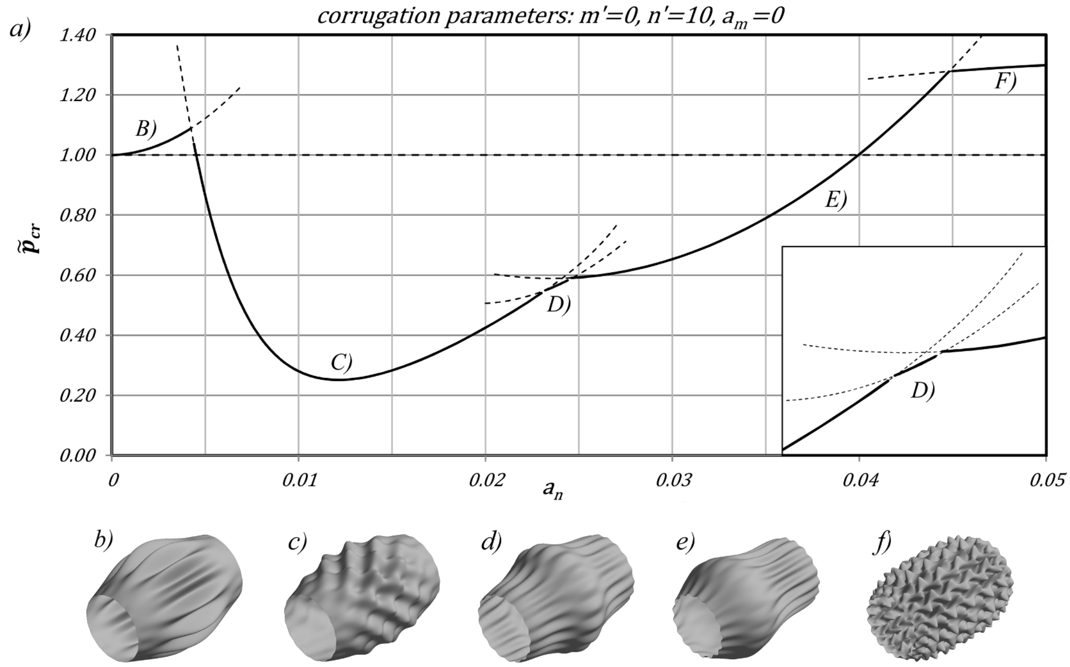

Fig. 6. Examples of buckling modes of circumferentially corrugated barrelled shells. Change in relative critical load a); curves corresponding to the buckling modes: B)–F), buckling modes: b)–f).

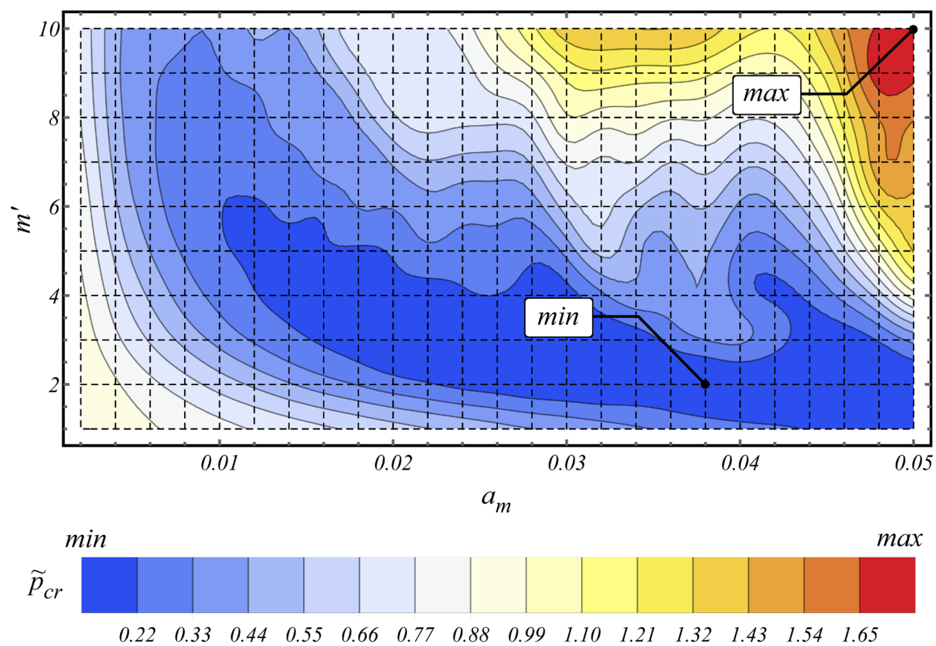

Fig. 7. Relative critical load $\tilde{p}_{cr}$ for barrelled shells corrugated in meridional direction.

shells it is appropriate to perform calculations for half of the digital model by implementing symmetry boundary conditions. This is because buckled shell is expected to maintain the symmetry with respect to the *yz* plane. However, such phenomenon does not apply to numerous cases of corrugated shells, leading to inflated values of critical load, thus whole model must be considered. The number of finite elements changes with type of the shell and the values of corrugation parameters, similarly to the thickness t. Example of meshed corrugated barrelled shell is presented in Fig. 5.

Meaningful part of structural stability analysis is observation of buckled structures. The shapes of buckled smooth shells have usually a form of one meridional half-wave and few circumferential full-waves. Examples of the buckling modes for the selected corrugated shell are presented in Fig. 6. Relative critical load $\tilde{p}_{cr}$ is analysed in a function of dimensionless amplitude a_n. Each buckling mode is represented by one, continuous curve. Intersection of the neighbouring curves correspond to such a_n values, for which buckling mode changes. Dashed part of each curve represents the same buckling mode, however those parts cannot be considered as $\tilde{p}_{cr}$. The reason for that is the presence of another curve (buckling mode) for which buckling load has the lowest value, which is the definition of the critical load. Buckling modes of corrugated shells may significantly vary from the smooth ones. Those represent various, often unpredictable forms of stability loss, including: serious irregularity, local bucking, multiple half-waves along meridional direction, and loss of the initial symmetry.

Despite the fact results are not expected to form continuous

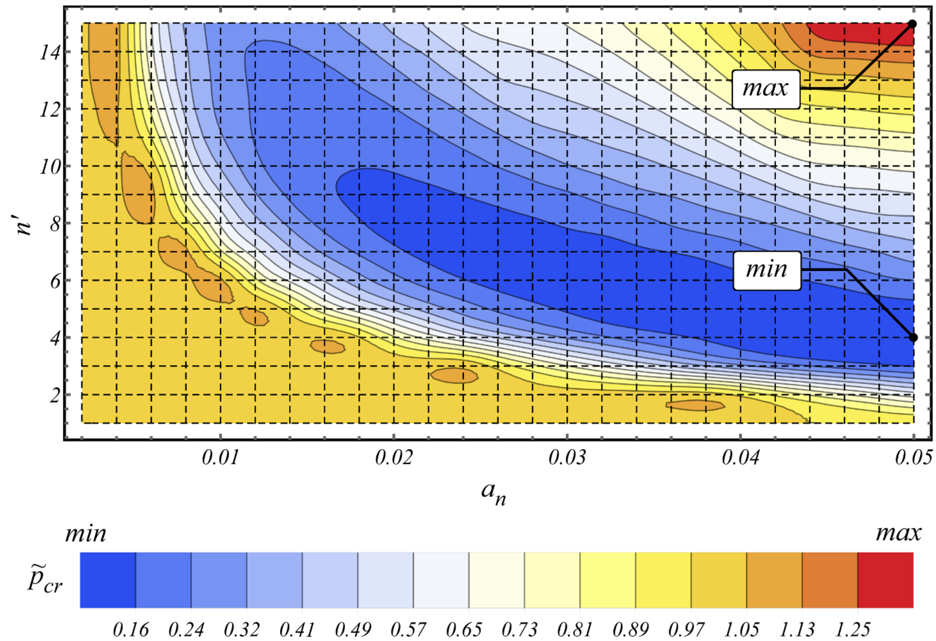

Fig. 8. Relative critical load $\tilde{p}_{cr}$ for barrelled shells corrugated in circumferential direction.

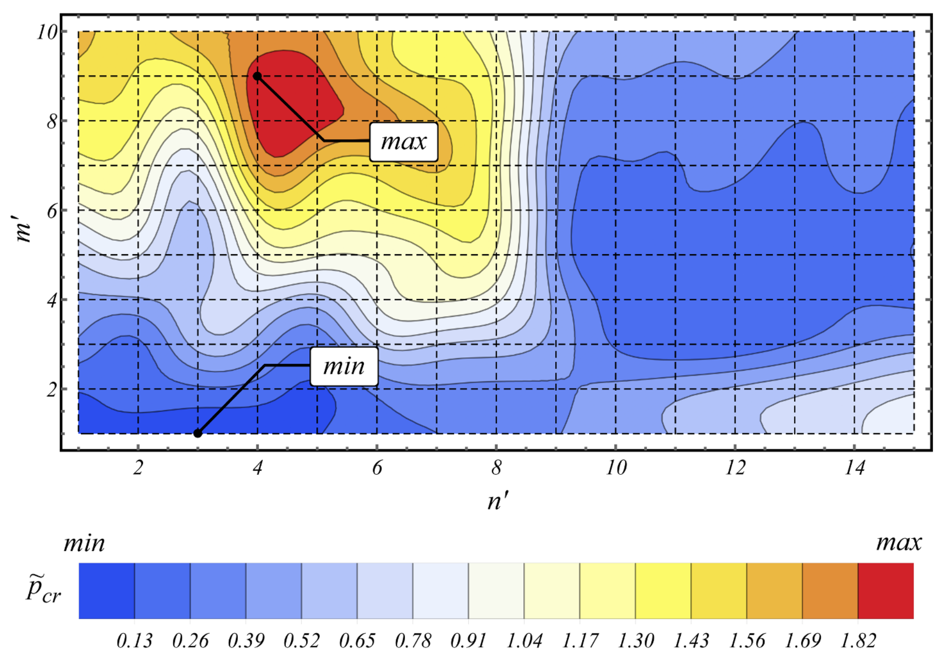

Fig. 9. Relative critical load $\tilde{p}_{cr}$ for barrelled shells corrugated in both principal directions.

functions of corrugation parameters e.g. $\tilde{p}_{cr}(m', a_m)$, for the sake of presentation complete results for three of nine analysed shells are presented in contour graphs in Figs. 7–9 Mentioned graphs are based on values of $\tilde{p}_{cr}$ evaluated for corrugation parameters denoted in Eq. (16) and concern barrelled shell with all possible forms of the corrugation. Evaluated values of relative critical load correspond to the points at the intersection of dashed lines. Relative critical load $\tilde{p}_{cr}$ presented in Fig. 8 includes those given in Fig. 6, however latter were strictly analysed by performing additional simulations to precisely distinguish the values of dimensionless amplitude a_n for which the change of buckling mode occurs. Such change takes place at the intersection of neighbouring curves. Contour plots Figs. 7–9 do not necessarily include those points, therefore those may not contain some interesting values of $\tilde{p}_{cr}$ e.g. *B*) and *C*) curves intersection from Fig. 6. As it is expected, the values of relative critical load $\tilde{p}_{cr}$ significantly vary with corrugation parameters.

Extreme values of relative critical load: $\tilde{p}_{cr\ max}$ and $\tilde{p}_{cr\ min}$ based only on specified corrugation parameters are denoted in Figs. 7–9. Similar contour graphs were created for six remaining cases. For most of them buckling modes change rapidly with corrugation parameters, hence distinguishing all of them is nearly impossible. To summarize performed FEM studies the corrugated shells with the greatest value of critical load $\tilde{p}_{cr\ max}$ and their parameters are presented in Tables 3–5. For every considered corrugated shell, there are specific corrugation parameters leading to increased critical load comparing to the smooth shell of the same type. The highest value of $\tilde{p}_{cr\ max}$ occurs for cylindrical shell corrugated in the meridional direction $\tilde{p}_{cr\ max} = 14.923$. However, such critical loads were achieved mostly for maximum values of corrugation parameters. Due to that fact, broadening range of those parameters could lead to even greater $\tilde{p}_{cr\ max}$ values.

Table 3
Linear buckling analysis summary for corrugated barrelled shells.

Type of shell	Barrelled		
Direction of corrugation	Meridional	Circumferential	Meridional and circumferential
$\tilde{p}_{cr\ max}$	1.757	1.299	1.893
Corrugation parameters	$m' = 10$, $a_m = 0.05$	$n' = 15$, $a_n = 0.05$	$m' = 9$, $n' = 4$
Thickness t [mm]	2.085	2.164	2.107
Initial shape	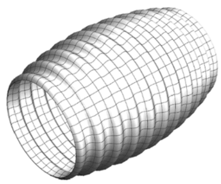	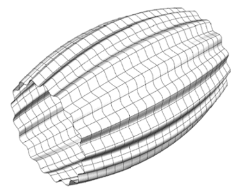	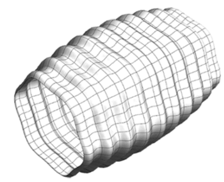
Buckled shape		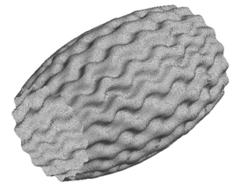	

Table 4
Linear buckling analysis summary for corrugated pseudo-barrelled shells.

Type of shell	Pseudo-barrelled		
Direction of corrugation	Meridional	Circumferential	Meridional and circumferential
$\tilde{p}_{cr\ max}$	5.675	5.632	6.162
Corrugation parameters	$m' = 10$, $a_m = 0.042$	$n' = 8$, $a_n = 0.05$	$m' = 2$, $n' = 15$
Thickness t [mm]	3.441	3.480	3.019
Initial shape	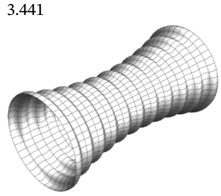	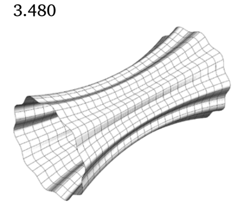	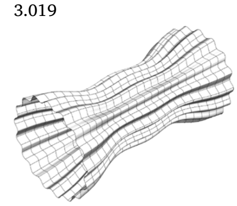
Buckled shape			

5. Nonlinear buckling

Presented previously linear (eigenvalue) buckling analysis is appropriate for a stability problem only when behaviour of a loaded structure meets particular conditions. Foremost, it is assumed that negligible deformations occur before buckling. Additionally, a structure is characterised by linear load-deformation response. Critical loads calculated as eigenvalues are located on the initial load-deformation path, as the stiffness matrix of the structure is assumed constant prior to stability loss. Above assumptions are justified only for particular structures with relatively simple geometry. Furthermore, while performing eigenvalue buckling analysis it is impossible to study initial geometrical imperfections influence and predict post-buckling behaviour. It is well known issue that critical loads calculated in nonlinear buckling analysis have lower values than those obtained in eigenvalue buckling at least for the classic shells. Considering complex shape of the analysed shells, eigenvalue buckling analysis might be insufficient. To study their structural behaviour profoundly nonlinear buckling analysis must be performed.

While performing nonlinear buckling analyses the most essential problem is to obtain equilibrium path for a structure. Such load-displacement response allows one to evaluate the critical load in more realistic manner, where assumptions made on behalf of the eigenvalue buckling are omitted. As most of the shell structures are known for their unstable equilibrium paths, critical load can be considered to be the first maximum load on the load-displacement curve. Due to that the equilibrium path must include the state when the structure is unstable i.e. post-buckling behaviour. Ansys software enables to analyse nonlinear buckling in multiple ways. If the unstable state is to be analysed, the most appropriate is to use arc-length method. Nonlinear buckling analyses are undoubtedly time consuming and computationally demanding. Additionally when geometry of the structure is complicated

Table 5
Linear buckling analysis summary for corrugated cylindrical shells.

Type of shell	Cylindrical		
Direction of corrugation	Meridional	Circumferential	Meridional and circumferential
$\tilde{p}_{cr\ max}$	14.923	3.491	12.354
Corrugation parameters	$m' = 10$, $a_m = 0.05$	$n' = 15$, $a_n = 0.05$	$m' = 10$, $n' = 3$
Thickness t [mm]	2.600	2.583	2.569
Initial shape	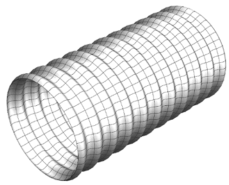	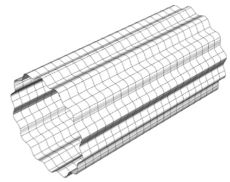	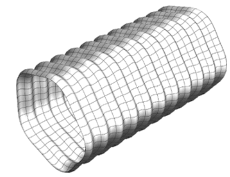
Buckled shape		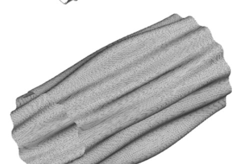	

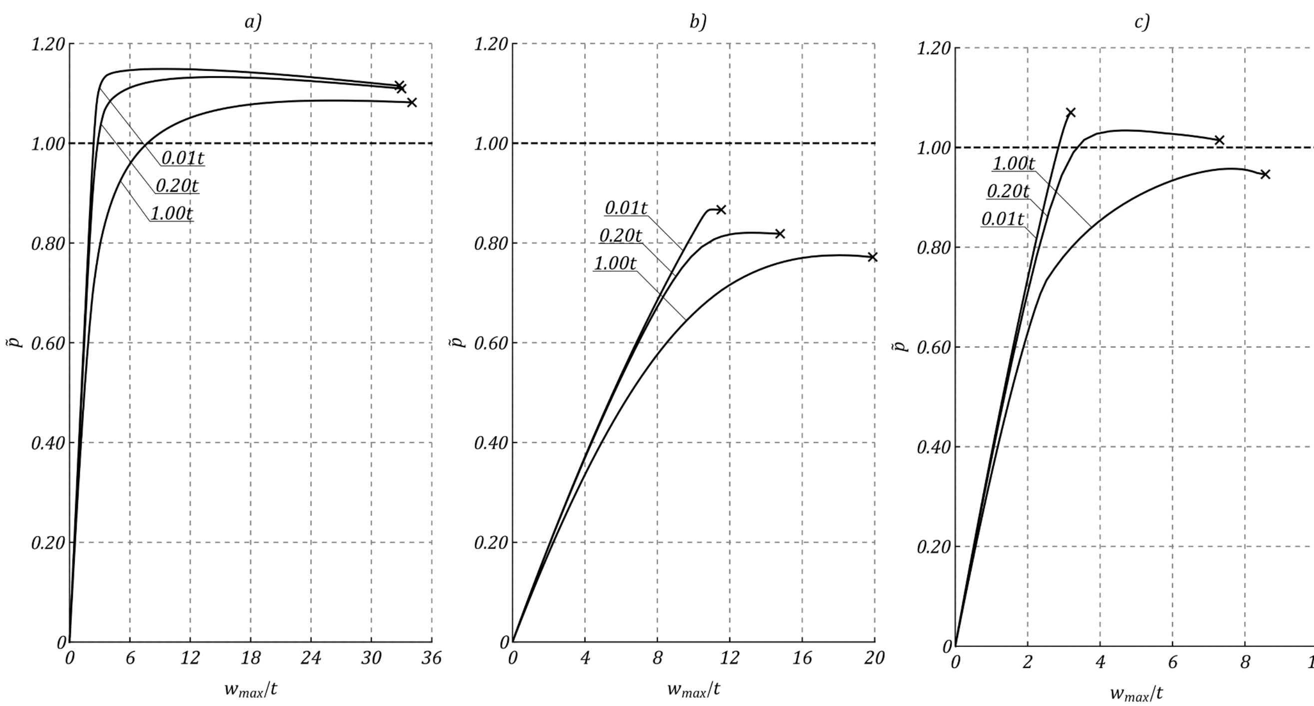

Fig. 10. Equilibrium paths for barrelled shells corrugated in: a) meridional direction, b) circumferential direction, c) both directions.

and post-buckling behaviour is to be analysed, the problem can become unmanageable even using FEM. Possibility of solving such problem depends on the details of the nonlinear numerical analysis e.g.: convergence criteria, FE model, maximum number of iterations at each time step, arc-length controls, initial imperfections. Having that in mind, the problem is reduced to the corrugated shells with the greatest value of critical load $\tilde{p}_{cr\ max}$ evaluated in the eigenvalue buckling analysis (Tables 3–5). Imperfections are considered in the form of the first buckling mode. The three maximum values of deviation from the prefect geometry are considered $w = 0.01t,\ 0.20t,\ 1.00t$. Applied load is defined as a dimensionless parameter in following manner

$$\tilde{p} = \frac{p}{p_{cri}} \tag{17}$$

where p – applied pressure, p_{cri} – critical load of the shell with particular corrugation parameters obtained in linear buckling.

The numerical analysis is stopped when applied load reduces in a function of maximum value of displacements, so the stability loss is evident. The second criteria for terminating the analysis is when applied load reaches the maximum of 150% of the buckling load obtained in linear buckling analysis. Importantly, in some cases, termination is caused by the convergence problem of the solver, when the structure becomes unstable. Considering such issue, for selected shells obtained solution was additionally verified using force method, which confirmed the results from arc-length method in the stable state. In all of the presented results, displacements significantly exceed thickness of the analysed shells. However, due to some convergence issues and relatively small number of analysed shells, performed nonlinear buckling analyses can be considered preliminary and might require further studies.

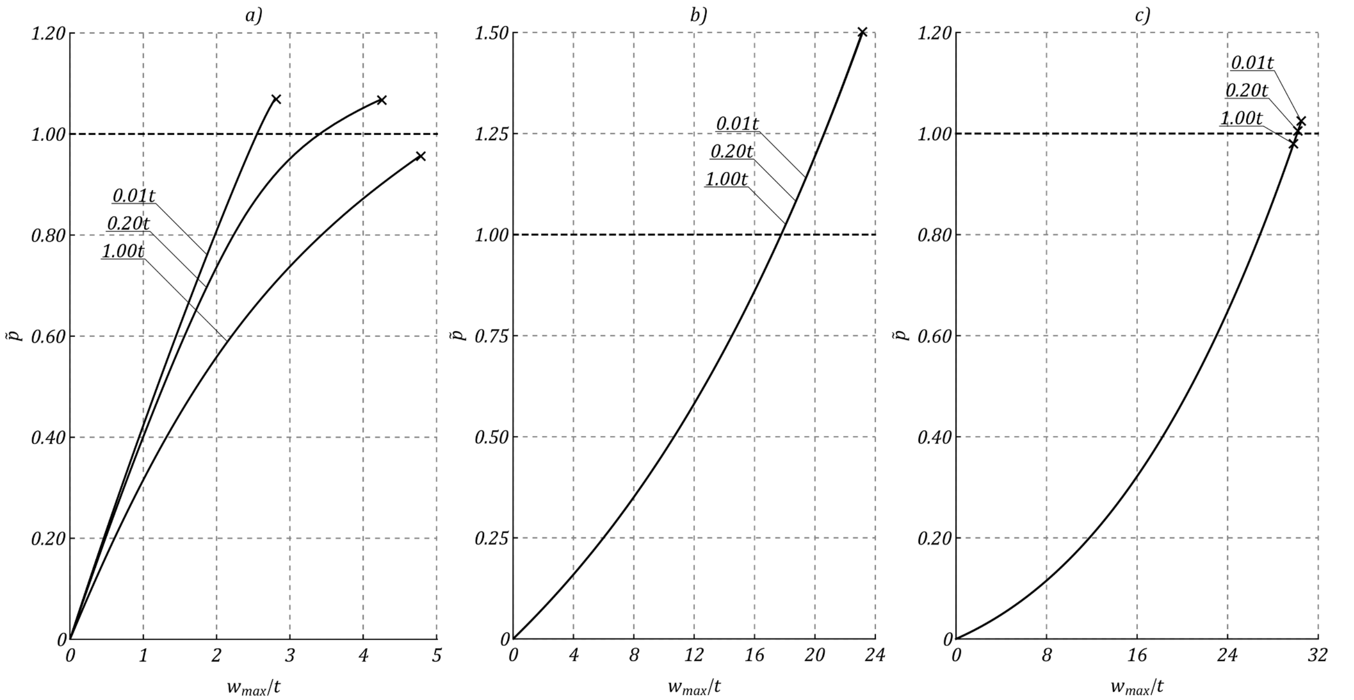

Fig. 11. Equilibrium paths for pseudo-barrelled shells corrugated in: a) meridional direction, b) circumferential direction, c) both directions.

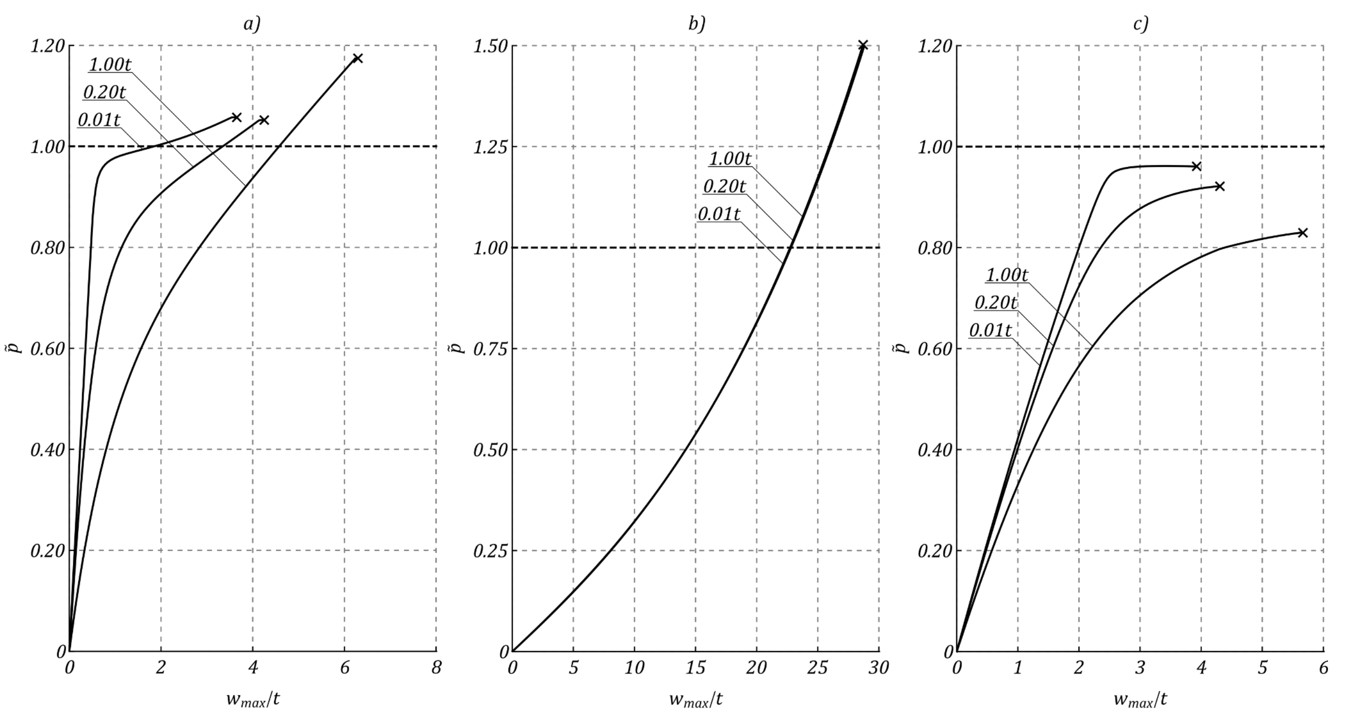

Fig. 12. Equilibrium paths for cylindrical shells corrugated in: a) meridional direction, b) circumferential direction, c) both directions.

The presented nonlinear buckling results (Figs. 10–12) shows that structural behaviour of corrugated shells may vary from the standard smooth shells. It is evident for shells corrugated in circumferential direction. Those structures are greatly elastic, which results in extreme deformations, even for relatively low values of the applied load.

Pseudo-barrelled (Fig. 11) and cylindrical (Fig. 12) shells do not lose stability in the prescribed load range and their load-deformation response can be considered initially nonlinear, despite magnitude of the imperfections. The shells corrugated in the meridional direction are characterised by the similar behaviour to the classic, smooth shells. In case of the cylindrical shells (Fig. 12) corrugated in the meridional direction, stabilization of the equilibrium path is observed. Comparing those shells with the shells corrugated in both directions, it is essential that deformations significantly increase for the latter. The influence of imperfections depends on type of the structure. It generally leads to an increase in the deformations and lower value of the critical load. Some shells are not sensitive for initial imperfections, most likely due to the magnitude of deformations. The example of such structure is pseudo-barrelled shell corrugated in the circumferential direction (Fig. 11).

From the presented nonlinear buckling analyses it is evident, that linear buckling analysis is insufficient in case of the structures with such complex geometry. As it is shown, the critical load obtained in the linear buckling analysis does not match with the nonlinear buckling. Importantly, obtained in nonlinear buckling critical load for a structure can be significantly greater or lower. Undoubtedly further studies for corrugated shells are required to investigate the post-buckling behaviour. The most essential issue is to determine appropriate convergence criteria for the solver while using the arc-length method.

6. Conclusions

Development in technical areas requires finding new, more efficient solutions. One possible method of achieving improved load-carrying ability of the shell structures is modification of their geometry. In this work corrugation of the middle surface is considered. Such structures can serve as pressure vessels, liquid storage tanks (draining process), underground tanks, cores of multi-layered shells, hulls of submersible vehicles, silos, road culverts and civil engineering structures. Assumed values of geometrical parameters correspond to industrial pressure vessels and liquid storage tanks. The thickness remains relatively small to obtain lightweight structures with significantly greater load-carrying ability than smooth shells. Analysed modification of geometry is controlled by the corrugation parameters: number of full-waves in circumferential direction, number of half-waves in meridional direction, and their amplitudes. By applying adequate thickness of the shell the mass remains constant. Critical load obtained from the linear buckling analysis of such shells is compared to the smooth shells. The study is based on FEM linear and nonlinear buckling analysis using Ansys software.

Inspecting the results of the linear buckling analysis one may conclude that specific ranges of corrugation parameters lead to the significant increase of the critical load values for all of the analysed types of shells. The greatest improvement in critical load $\tilde{p}_{cr\ max} = 14.923$ is observed for the cylindrical shell corrugated in the meridional direction. For barrelled and pseudo-barrelled shells the most efficient modification is the corrugation in the both principal directions. For all considered shells the lowest values of the maximum relative critical load $\tilde{p}_{cr\ max}$ are noted for circumferential corrugation. Analysing summarized results in Tables 3–5, one may conclude that in general, corrugation has the greatest effect on the cylindrical shells and the least for the barrelled structures. In addition, considering relative small values of the corrugation amplitudes, presented geometries may represent shells with initial imperfections. The common knowledge is that the geometrical imperfections lead to decreased value of the critical loads of shells. Performed numerical calculations show, that some particular imperfections may increase critical load value. Such phenomenon is shown in Fig. 6.

Nonlinear buckling analysis concludes that linear buckling is insufficient to evaluate the critical load of such geometrically complex structures. Performed analyses demonstrate that stability loss can occur for lower or greater load than the critical load obtained in the linear buckling. With current possibilities of FEM software, analysing post-buckling behaviour becomes quite simple for the classic, smooth shells. Nonetheless, modification of their middle surface in form of the corrugation leads to the significant difficulties in nonlinear buckling analysis while using arc-length method. Regardless results discrepancies between linear and nonlinear buckling, the study shows that corrugated shells are able to carry significantly higher loads than the smooth shells for assumed boundary conditions, while maintaining their initial mass.

Results of the presented study may be the basis to develop the more efficient structures. However, due to their complex spatial shape, most of the considered shells are unable to manufacture in conventional methods. As additive manufacturing technologies being currently extensively studied and developed, the possibility of manufacturing more complex shapes of shell structures grows drastically. Despite the technological limitations, corrugated shells are interesting and efficient structures whose load-carrying ability significantly exceeds ability of the smooth shells. To fully understand the structural nature of the corrugated shells it is necessary to additionally consider problem of stress distribution and to extend the post-buckling analysis. Having that in mind, presented topic remains vital and open for further studies.

Acknowledgement

The author is greatly thankful to Prof. Krzysztof Magnucki and Dr. Paweł Jasion for providing valuable consultations, related to the presented work.

The paper is developed based on the statutory activity of the Poznan University of Technology funded with grants (Grant no 02/21/DSPB/3514) for education allocated by the Ministry of Science and Higher Education in Poland.

References

[1] Volmir AS. Stability of deformable systems. Moscow: Nauka; 1967.
[2] Bushnell D. Computerized buckling analysis of shells. Dordrecht, Boston, Lancaster: Martinus Nijhoff; 1985.
[3] Ventsel E, Krauthammer T. Thin plates and shells. Theory, analysis and applications. New York, Basel: Marcel Dekker, Inc; 2001.
[4] Jasion P. Buckling and post-buckling analysis of shells of revolution with positive and negative Gaussian curvature, Rozprawy nr 530. Poznan: Wydawnictwo Politechniki Poznańskiej; 2015.
[5] Magnucki K, Stawecki W. Stateczność wybranych części konstrukcji. Poznan: Instytut Pojazdów Szynowych TABOR; 2016.
[6] Xue J, Hoo Fat MS. Buckling of a non-uniform, long cylindrical shell subjected to external hydrostatic pressure. Eng Struct 2002;24:1027–34.
[7] Błachut J, Smith P. Buckling of multi-segmented underwater pressure hull. Ocean Eng 2008;35:247–60.
[8] Wunderlich W, Albertin U. Buckling behaviour of imperfect spherical shells. Int J Non Linear Mech 2002;37(4–5):589–604.
[9] Magnucki K. Post-buckling behaviour of an open sandwich conical shell. Arch Mech Eng 1980;27(4):397–409.
[10] Paczos P, Zielnica J. Stability of orthotopic elastic-plastic open conical shells. Thin-Walled Struct 2008;48(5):530–40.
[11] Jasion P, Magnucki K. Elastic buckling of horizontal barrelled shells filled with liquid – numerical analysis. Thin-Walled Struct 2012;52:117–25.
[12] Łukasiewicz S, Szyszkowski W. On the stability and the post-buckling equilibrium of shells of revolution. J Appl Math Mech 1971;51:635–9.
[13] Jasion P, Magnucki K. Theoretical investigation of the strength and stability of special pseudo-spherical shells under external pressure. Thin-Walled Struct 2015;93:88–93.
[14] Zhang M, Tang WX, Wang F, Zhang J, Cui WC, Chen Y. Buckling of bi-segmented spherical shells under hydrostatic external pressure. Thin-Walled Struct 2017;120:1–8.
[15] Zingoni A, Mokhothu B, Enoma N. A theoretical formulation for the stress analysis of multi-segmented spherical shells for high-volume liquid containment. Eng Struct 2015;87:21–31.
[16] Jasion P, Magnucki K. Elastic buckling of clothoidal-spherical shells under external pressure – theoretical study. Thin-Walled Struct 2015;86:18–23.
[17] Zhang J, Wang ML, Cui WC, Wang F, Hua ZD, Tang WX. Effect of thickness on the buckling strength of egg-shaped pressure hulls. Ships Offshore Struct 2018;13(4):375–84.
[18] Zingoni A. Liquid-containment shells of revolution: A review of recent studies on strength, stability and dynamics. Thin-Walled Struct 2015;87:102–14.
[19] Kar VR, Panda SK. Post-buckling behaviour of shear deformable functionally graded curved shell panel under edge compression. Int J Mech Sci 2016;115–116:318–24.
[20] Kar VR, Mahapatra TR, Panda SK. Effect of different temperature load on thermal postbuckling behaviour of functionally graded shallow curved shell panels. Compos Struct 2017;160:1236–47.
[21] Malinowski M, Belica T, Magnucki K. Buckling of sandwich cylindrical shell with corrugated main core and three layer faces. Appl Comput Sci 2014;10:18–25.
[22] Iwicki P, Sondej M, Tejchman J. Application of linear buckling sensitivity analysis to economic design of cylindrical steel silos composed of corrugated sheets and columns. Eng Fail Anal 2016;70:105–21.
[23] Iwicki P, Wójcik M, Tejchman J. Failure of cylindrical steel silos composed of corrugated sheets and columns and repair methods using a sensitivity analysis. Eng Fail Anal 2011;18:2064–83.
[24] Jongpradist P, Rojbunsongsri R, Kamnerdtong T, Wongwises S. Parametric study and optimisation of a food can corrugation design using a response surface method. J Mech Sci Technol 2013;27(7):2043–52.
[25] Dickson JN, Brolliar RH. The general instability of ring-stiffened corrugated cylinders under axial compression, NASA TN D-3089. Washington: National Aeronautics and Space Administration; 1966.
[26] Liu ZF, Hao WQ, Xie JM, Lu JS, Huang R, Wang ZH. Axial-impact buckling modes and energy absorption properties of thin-walled corrugated tubes with sinusoidal patterns. Thin-Walled Struct 2015;94:410–23.

[27] Hao WQ, Xie JM, Wang FH, Liu ZF, Wang ZH. Analytical model of thin-walled corrugated tubes with sinusoidal patterns under axial impacting. Int J Mech Sci 2017;128–129:1–16.
[28] Hao WQ, Xie JM, Wang FH. Theoretical prediction of the progressive buckling and energy absorption of the sinusoidal corrugated tube subjected to axial crushing. Comput Struct 2017;191:12–21.
[29] Ghazijahani TG, Dizaji HS, Nozohor J, Zirakian T. Experiments on corrugated thin cylindrical shells under uniform external pressure. Ocean Eng 2015;106:68–76.
[30] Ning X, Pellegrino S. Imperfection-insensitive axially loaded thin cylindrical shells. Int J Solids Struct 2015;62:39–51.
[31] Malek S, Ochsendorf J, Wierzbicki T. The effect of double curvature on the Structural Capacity of Corrugated Gridshells. Wroclaw: Proceedings of the International Association for Shell and Spatial Structures (IASS) Symposium 2013 "BEYOND THE LIMITS OF MAN"; 2013.
[32] Malek S, Williams C. The equilibrium of corrugated plates and shells. Nexus Netw J 2017;19:619–27.
[33] CEN, EN 1993-1-6:2007 Eurocode 3, Design of steel structures – Part 1-6: Strength and Stability of Shell Structures. Brussels: CEN; 2007.